

# Evaluation of local and global ductility relationships for seismic assessment of regular masonry-infilled reinforced concrete frames using a coefficient-based method

R.K.L. Su\*, T.O. Tang and C.L. Lee

*Department of Civil Engineering, The University of Hong Kong,  
Pokfulam Road, Hong Kong, People's Republic of China*

*(Received August 31, 2012, Revised February 10, 2013, Accepted February 28, 2013)*

**Abstract.** Soft storey failure mechanism is a common collapse mode for masonry-infilled (MI) reinforced concrete (RC) buildings subjected to severe earthquakes. Simple analytical equations correlating global with local ductility demands are derived from pushover (PO) analyses for seismic assessments of regular MI RC frames, considering the critical interstorey drift ratio, number of storeys and lateral loading configurations. The reliability of the equations is investigated using incremental dynamic analyses for MI RC frames of up to 7 storeys. Using the analytical ductility relationship and a coefficient-based method (CBM), the response spectral accelerations and period shift factors of low-rise MI RC frames are computed. The results are verified through published shake table test results. In general applications, the analytical ductility relationships thus derived can be used to bypass the onerous PO analysis while accurately predicting the local ductility demands for seismic assessment of regular MI RC frames.

**Keywords:** local ductility; global ductility; coefficient-based method; confined masonry; soft storey; nonlinear analysis; period lengthening

---

## 1. Introduction

Low-rise masonry-infilled (MI) reinforced concrete (RC) frames, particularly 6- to 7-storey frames (Su and Zhou 2009), have been prevalent in developing countries because of low construction cost, even though they are vulnerable to seismic events (Rodríguez 2005, Terán-Gilmore *et al.* 2009, Dolšek and Fajfar 2001). These buildings are often constructed with bare frames having a larger clear height at the ground floor to accommodate commercial usage, whereas the upper storeys are partitioned for residential usage resulting to higher strength and stiffness. When the building is subjected to strong ground shaking and the lateral strength at the ground floor is inadequate to resist the seismic loads, lateral deformation will concentrate there.

Fig. 1(a) shows a notable drift concentrated at the soft storey after the Sichuan Earthquake in 2008. Soft storey failures occur when the interstorey drift ratio (IDR) demand exceeds the corresponding capacity, which Fig. 1(b) shows a total collapse of the soft storey. Besides buildings of discontinuous strength and stiffness, previous earthquakes and extensive studies (Dolšek and

---

\*Corresponding author, Associate Professor, E-mail: [klsu@hku.hk](mailto:klsu@hku.hk)

Fajfar 2001, Kwan and Xia 1996) revealed that even for the buildings with a uniform vertical distribution of infill, soft storey can be formed at the bottom floors if the ground motion is strong enough. In view of the severe damage often associated with the soft storey failure (Sucuoglu and Yazgan 2003), it is vital to assess their seismic performance, in particular the seismic response of non-seismically designed building stocks.



Fig. 1 Damages to masonry buildings in 2008 Sichuan Earthquake: (a) significant drift concentration at the first storey and (b) soft-storey failure at the first storey (China Academy of Building Research 2008)

Among different available seismic assessment methods, it is well-recognised that detailed nonlinear dynamic analyses can provide the most comprehensive information for the seismic assessment of buildings under inelastic response. However, the difficulty in obtaining a representative and full range of material properties, the cumbersome numerical modelling, and the lengthy computational time required for a representative ensemble of ground motion inputs hinder the practical use of nonlinear dynamic analysis. Furthermore, endless efforts could be spent on the seismic evaluation of a huge number of existing buildings liable to substandard construction due to the increase in seismic fortification levels.

Alternatively, a coefficient-based method (CBM) can provide a simplified means to assess manually the structural integrity of a building by evaluating the roof displacement or response spectral displacement (RSD) under seismic loads. The CBM serving as a preliminary assessment method for buildings has been extensively studied (e.g., Miranda 1999, Miranda and Reyes 2002, Gupta and Krawinkler 2000, Lu *et al.* 2009, Zhu *et al.* 2007, Tsang *et al.* 2009, Fardipour *et al.* 2011), but the assessment of the vulnerability of MI RC buildings has received limited attention until recently when the availability of more experimental studies of MI RC structures (e.g., Kwan and Xia 1996, Tomaževič and Klemenc 1997, Dolce *et al.* 2005, Kakaletsis and Karayannis 2008) have provided more empirical data for subsequent studies of simplified analyses (Su and Zhou 2009, Ruiz-García and Negrete 2009, Terán-Gilmore *et al.* 2009, Lee and Su 2012, Su *et al.* 2012), which will be elaborated in the later sections.

Before discussing those existing simplified analyses for MI RC frames, it is important to understand why existing CBMs derived for typical buildings cannot be employed directly to this type of buildings. Such problem is attributed to a conversion formula describing the deformation

demand relationships between the equivalent single-degree-of-freedom (SDOF) system and the critical local member of the multiple-degree-of-freedom (MDOF) structure, in which the deformation demand is usually presented in terms of dimensionless ductility. An accurate prediction of the relationship between the global ductility demand (the ductility demand of an equivalent bilinear SDOF building system) and the local ductility demand (the maximum storey IDR to the yield IDR of that storey) is crucial to the seismic performance evaluation, in which IDR is defined as the interstorey lateral displacement normalised by the storey height. For a building with known yield strength, the global ductility demand can be calculated from the CBM and the inelastic spectra (Ruiz-García and Miranda 2003, Terán-Gilmore *et al.* 2009) based on the capacity spectrum method (CSM). With this relationship, the local deformation demand can be derived and compared with the codified limits. Alternatively, the global ductility capacity can also be evaluated from this relationship if the local ductility factor at a particular performance level can be identified through experiments or codified limits.

Such a simple ductility-based relationship is especially advantageous to enable the CBM to be used as a rapid assessment tool for MI RC buildings, bypassing the onerous pushover (PO) analysis stipulated in typical standards (ATC-40, FEMA 356, FEMA 440). This simplified drift-based assessment is intended to supplement the rigorous and codified nonlinear static procedures (NSP) for quick seismic assessment of buildings. The buildings at seismic risk can thus be easily identified.

Among the CBMs proposed by different researchers, the ductility-based relationship has been generalised by various methods. Miranda (1999) and Miranda and Reyes (2002) studied medium- to high-rise steel moment resisting frame buildings using a drift factor ( $\beta_2$ ) to express the ratio of the maximum IDR to the roof drift ratio at a linear elastic state. Another drift factor ( $\beta_4$ ), which accounted for the concentration of IDR during a nonlinear state, was obtained by regression of the computational results from a PO analysis (Miranda 1996, Collins *et al.* 1996) of the building models based on the strong-column-weak-beam failure mechanism. Miranda and Reyes (2002) found that the drift factor,  $\beta_4$ , was affected by four primary factors comprising the number of storeys, failure mechanism, the level of inelastic deformation and the ground motion. However, their proposed drift factors are not applicable to buildings with a soft storey mechanism and a high IDR demand concentrated at a particular storey.

Gupta and Krawinkler (2000) developed a relationship between the inelastic IDR demand and the first mode response spectral displacement of MDOF steel frame buildings with several factors that account for the nonlinearity and the MDOF effects. The ratio of peak roof drift demands to IDR demands was found to be strongly dependent on the number of storeys and the ground motion characteristics. A constant drift factor of 1.2 was proposed for this ratio to account for low-rise buildings exposed to the earthquakes studied. However, the proposed factor might not apply to buildings with different numbers of storeys and/or soft storey effect, as a constant factor exists only when no deformation concentrates at the IDR with increasing ductility demands.

Zhu *et al.* (2007) proposed a simplified CBM to evaluate the maximum IDR of coupled shear wall structures. These researchers' study focused on medium- to high-rise regular RC frame and/or shear wall buildings. The equal displacement principle was used to simplify the calculation of the inelastic deformations. Similarly, Fardipour *et al.* (2011) proposed simple expressions to estimate the maximum IDR from the building height and maximum RSD from design spectra. However, both studies are only valid for tall buildings with natural periods larger than the second corner period of the design spectrum to comply with the use of the equal displacement principle; otherwise, their proposed drift factors are only suitable for elastic deformations.

Recent studies showed the improved adaptability of the CBM to seismic evaluation of low-rise MI RC buildings. Assuming the domination of the first vibration mode in PO analysis, Ruiz-García and Negrete (2009) suggested determining the inelastic drift demand of the first storey from the RSD at the inelastic state together with a normalised participation factor. Similarly, Terán-Gilmore *et al.* (2009) suggested estimating the local drift demands by the PO analysis until the target displacement based on a proposed modified wide-column model. Most recently, Lee and Su (2012) and Su *et al.* (2012) proposed a CBM to assess the spectral acceleration capacity (or the inherent strength) of low-rise MI RC buildings under the soft storey failure mechanism. Drift factors at the peak load state of low-rise MI RC buildings were calibrated using limited experimental information for 2- to 5-storey buildings. The empirical nature of the drift factors hinders the extension of the drift factors to similar but taller MI RC buildings. In addition, none of the above-mentioned studies has proposed theoretical models to justify existing empirical correlation between the critical IDR and the inelastic RSD demand.

In view of the above limitations, nonlinear PO analysis is employed in this study to evaluate the full range drift factors applicable to 3- to 7- storey regular MI RC frames with soft storey failure mechanisms. Simple analytical relationships of the global and local ductility demands are derived. The reliability of such relationships is tested using incremental dynamic analyses (IDA), which allows them to be verified in consideration of various ground motions and intensities, and the available experimental information. The proposed relationships allow the CBM to be extended to the evaluation of IDR demands in MI RC frames of up to 7 storeys in height.

## 2. Ductility demand relationships

### 2.1 Existing ductility relationship for low-rise MI RC buildings

The available ductility demand relationships that depend on the RSD and the global ductility demand are described in this section. The RSD of an equivalent SDOF obtained from the PO curve of a MDOF building is expressed in terms of the lateral roof displacement following the convention of the CSM in ATC-40, or FEMA 356 as

$$RSD = \frac{1}{\Gamma_1} \frac{\Delta_{roof}}{\phi_{roof,1}} \quad (1)$$

where  $\Gamma_1$  is the modal participation factor for the first vibration mode,  $\phi_{roof,1}$  is the normalised amplitude at the roof level of the first mode shape and  $\Delta_{roof}$  is the lateral peak displacement at the roof. This expression is still approximately correct for structures at the inelastic state dominated by the first vibration mode. The global ductility in the inelastic state can be defined as

$$\mu_G = \frac{RSD_{inel}}{RSD_y} = \frac{(\Delta_{roof})_{inel}}{(\Delta_{roof})_y} \quad (2)$$

where the subscripts *y* and *inel* refer to the yield state and inelastic state, respectively.

For soft storey failures characterised by the insufficient strength of either the diagonal struts or the infill mortar joints, Paulay and Priestley (1992) proposed a simplified relationship for the

global and local ductility based on three assumptions: (1) all inelastic displacements are concentrated at the first storey, (2) a linear deflection profile can approximate the deformed shape above the first storey, and (3) the resultant seismic lateral load acts on a lumped mass at 2/3 of the building height. This ductility relationship is expressed as follows

$$\mu_G = \frac{1}{n}(\mu_L - 1) + 1 \quad (3)$$

where  $n$  is the number of storeys, and  $\mu_L (\geq 1)$  is the local ductility factor at the first storey. Even though Eq. (3) is a closed form expression, the assumed linear deformation shape above the first storey can deviate considerably from the actual deformation from PO deflections. This study quantifies the associated potential errors. The maximum number of storeys to which the expression can be applied will also be estimated.

## 2.2 Ductility relationships for the CBM

Assuming there is no premature tearing failure of floor diaphragms and/or tensile failure of tie columns, Su *et al.* (2011) derived the expressions for determining the RSD demand and response spectral acceleration (RSA) demand of MI RC buildings as follows

$$RSD = \frac{H_b \theta}{\lambda} \quad (4)$$

$$RSA = \frac{H_b}{T_0^2} \frac{(2\pi)^2}{\lambda} \frac{\theta}{\beta^2} \quad (5)$$

where  $\lambda$  is the drift factor,  $\theta$  is the maximum IDR demand at a specific performance state,  $H_b$  is the total height of the building,  $T_0$  is the initial fundamental period of the undamaged structure, and  $\beta$  is the period shift factor (PSF) that accounts for the lengthening of the fundamental period during inelastic deformation. In these researchers' study (Su *et al.* 2012), the parameters ( $\lambda$ ,  $\beta$ ,  $\theta$  and  $T_0$ ) used in Eqs. (4) and (5) were determined from shake table test results at the peak load state. Since MI RC buildings in low-to-moderate seismicity regions are more likely to survive in a rare earthquake because of the relatively low seismic demands, these drift related factors can be determined more reliably for buildings underwent limited inelastic behaviour. A considerably consistent range was attained for these parameters derived from four shake-table tests in the study of Su *et al.* 2012, whereas limited shake-table test results constrain the generality of these drift parameters. Conversely, based on analytical PO models, alternative close form expressions for deriving these parameters are described herein.  $\lambda$  and  $\beta$  can be expressed in terms of the maximum IDR, provided that the deflected shape of the buildings can be reasonably estimated. Following the ductility relationship proposed by Paulay and Priestley (1992),  $\lambda$  and  $\beta$  are expressed as follows

$$\lambda = \frac{3}{2} \cdot \frac{\mu_L}{\mu_G} = \frac{3}{2} \cdot \frac{n\mu_L}{(\mu_L - 1) + n} \quad (6)$$

$$\beta = \beta_i \beta_\mu = \beta_i \sqrt{\mu_G} = \beta_i \sqrt{\frac{1}{n}(\mu_L - 1) + 1} \quad (7)$$

where  $\beta_i (=T_i/T_0)$  is the PSF from the undamaged fundamental period ( $T_0$ ) to the idealised linear

period ( $T_i$ ), and depends on the idealised bilinear model used (see Section 3), and  $\beta_\mu (=T_{eff}/T_i)$  is the PSF from the idealised linear period ( $T_i$ ) to the effective period ( $T_{eff}$ ) in the inelastic state. Therefore, using Eqs. (4) to (7), the RSD or RSA demands associated with an IDR (or  $\theta$ ) at a particular performance state can be determined once  $\mu_L$ ,  $n$ , and  $\beta_i$  are known.

Using the elasto-perfect plastic assumption for the load-interstorey relationship, Eqs. (4) and (5) are rewritten as follows

$$RSD = \mu_G RSD_y \quad (8)$$

$$RSA = \frac{1}{T_0^2} \frac{(2\pi)^2}{\beta_i^2} RSD_y \quad (9)$$

Eq. (9) shows that RSA is inversely proportional to  $T_0^2$  and  $\beta_i^2$  and is directly proportional to the yield RSD. This equation further implies that the RSA demand is independent of the maximum IDR for elasto-perfectly plastic structural systems. If a linear deflection profile along the building height above the first storey in the inelastic state is postulated, the above equations are rewritten as follows

$$RSD = h\theta_y(\mu_L - 1) + \frac{2}{3}nh\theta_y \quad (10)$$

$$RSA = \frac{1}{T_0^2} \frac{(2\pi)^2}{\beta_i^2} \cdot \frac{2}{3}nh\theta_y \quad (11)$$

where  $h$  is the uniform interstorey height and  $\theta_y$  is the IDR at the yield state. Thus, the RSD or RSA demands at a particular local ductility demand,  $\mu_L$ , can be defined once the basic building properties  $n$ ,  $h$ , and  $T_0$  are available, and  $\beta_i$  and  $\theta_y$  have been obtained from the building's (global) bilinear force-displacement backbone curve.

### 2.3 Proposed ductility relationships

In this section, the ductility relationship proposed by Paulay and Priestley (1992) is analytically derived, taking into account the actual deformation shape of the buildings. Because the seismic responses of regular MI RC buildings are likely to be governed by the first vibration mode, the higher mode effects have been ignored in the PO analysis. An invariant rectangular or triangular external force distribution is applied to the building models throughout the entire (PO) loading process. The buildings are simulated by lumped mass models with uniform distributions of mass and stiffness along the height. Based on the PO analysis, the following analytical ductility relationships are generalised

$$\text{Rectangular load distribution: } \mu_G = 1 + \frac{2(\mu_L - 1)}{1 + n} \quad \text{for } n \geq 2 \quad (12)$$

$$\text{Triangular load distribution: } \mu_G = 1 + \frac{\mu_L - 1}{n - \sum_{i=1}^{n-1} \frac{(1+i)i}{2N}} \quad \text{for } n \geq 2, \quad (13)$$

where 
$$N = \frac{(1+n)n}{2} \tag{14}$$

To evaluate the RSA or RSD,  $\mu_G$  from Eq. (12) or Eq. (13) can be used in Eq. (8) or Eq. (9), respectively. To account for the deviation of the actual yielded deformation shapes from the idealised linear deformation shape (see Fig. 2),  $RSD_y$  in both RSD and RSA formulations is multiplied by an adjustment factor ( $\alpha_t$ ) that is a function of  $n$  (i.e., the number of storeys). Fig. 3 shows the exact and regression results of  $\alpha_t$  for 2- to 7-storey frames. For the triangular load distribution, the  $RSD_y$  and the adjustment factor is

$$RSD_y = \frac{2}{3}nh\theta_y \cdot \alpha_t \tag{15}$$

$$\alpha_t = -0.0014n^3 + 0.0305n^2 - 0.225n + 1.3968 \tag{16}$$

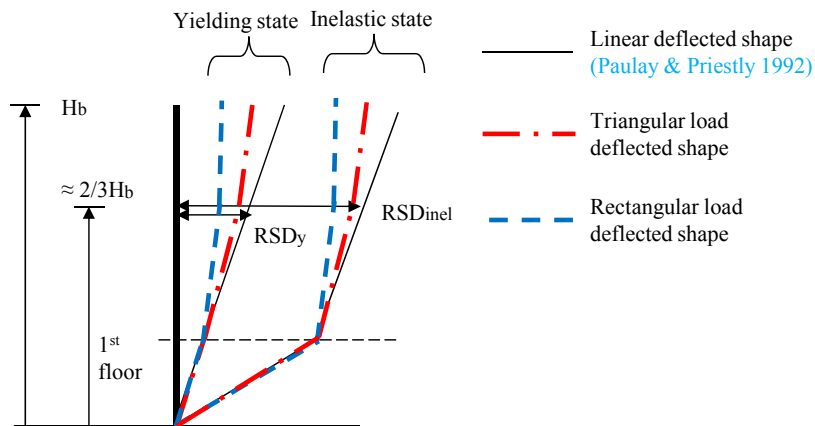


Fig. 2 Definitions of different deflected shapes at the yielding and inelastic states

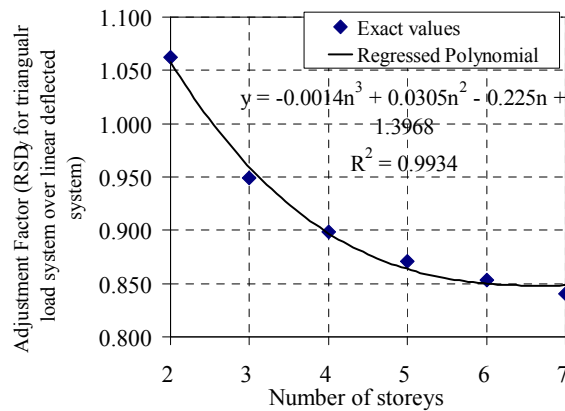


Fig. 3 Plot of adjustment factors against number of storeys to convert RSD at yield state from linear deflection system to triangular loading system

The statistical coefficient  $R^2$  factor as shown in Fig. 3 is equal to 0.9934, which is close to 1 indicating a good fit of data. The resulting values using these equations and comparison with the exact values by percentage are shown in Table 1. The reliability of Paulay and Priestley proposed (Equation 3) and the developed ductility relationships (Eqs. (12) and (13)) are compared using the IDA as described in the following sections.

### 3. Setup of numerical models

#### 3.1 Numerical models

In this study, 3-, 5-, and 7-storey MI RC frame models with a constant storey height of 3 m and a uniform storey mass of 100 tons, except for the roof level, which has a mass of 70 tons, are constructed for the IDA. The weight used in the model is comparable to a 2-bay, 9 m x 9 m low-rise MI RC building studied by Zheng *et al.* (2004). Because the effects of axial deformation on MI RC frames and rotational deformation at beam-column joints on the overall lateral deformation are negligible due to the relatively high rigidity for low-rise MI RC buildings, the lateral response is governed by shear deformations (Terán-Gilmore *et al.* 2009). A simplified, two-dimensional, lumped-mass stick model, assuming only the translational degree of freedom on each node, is used as shown in Fig. 4. The Bouc-Wen model (Wen 1976, Ma *et al.* 2004) is used to simulate the nonlinear storey restoring force response, which will be discussed in the next section.

Table 1 Adjustment factors to convert RSD at yield state from linear deflection system to triangular loading system

Number of storeys	Adjustment factor	% Error
2	1.058	-0.5
3	0.959	1.0
4	0.895	-0.4
5	0.859	-1.3
6	0.842	-1.3
7	0.836	-0.6

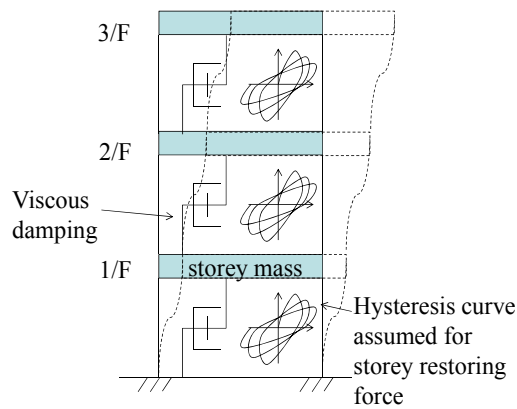


Fig. 4 Two-dimensional lumped mass stick model for MI RC buildings

For an  $n$ -storey building subjected to earthquake excitations, it is represented by the following equation of motion as (Foliente 1993)

$$\mathbf{M}\ddot{\mathbf{x}} + \mathbf{C}\dot{\mathbf{x}} + \mathbf{R}(\mathbf{x}) = -\mathbf{M}\mathbf{1}\ddot{u}_g + \mathbf{H}' \quad (17)$$

where  $\mathbf{M}$  is the mass matrix;  $\mathbf{x}$ ,  $\dot{\mathbf{x}}$ , and  $\ddot{\mathbf{x}}$  are the relative displacement, velocity and acceleration vectors to the ground, respectively;  $\mathbf{C}$  is the damping matrix obtained by assuming a modal damping ratio of 5% for each vibration mode;  $\mathbf{R}(\mathbf{x})$  is the storey restoring force matrix, which is a function of  $\mathbf{x}$  and other hysteretic parameters described in the Bouc-Wen model;  $\mathbf{1}$  is the unit column vector;  $\ddot{u}_g$  is the ground acceleration; and  $\mathbf{H}'$  is the equivalent incremental lateral force vector induced by the P-delta effect.

### 3.2 Hysteretic model of storey restoring forces

The hysteresis load-displacement behaviour of MI RC frames has been extensively studied. Among the reported studies, Kakaletsis and Karayannis (2008) tested 1/3-scale single bay and single-storey MI RC frame specimens under laterally reversed cyclic loading to examine the contributions of infill type and concentric opening to the force-displacement behaviour. All specimens with dimensions measuring 1500 mm in width and 1000 mm in height were prepared in accordance with Greek standards which are similar to Eurocodes. Among the two types of infill tested in that study, the specimen with stronger solid infill is selected to model the hysteretic behaviour here. The infill is designed to have lower lateral strength than columns to avoid brittle frame failure, whilst the RC frame is designed to be ductile. During the test, the nonlinear behaviour was initiated by the inclined cracking of the infill at the compression corners, and later was joined by horizontal sliding cracks along bed joints at the mid height of panel. Plastic hinges formed also at the top and bottom of the columns. The failure mechanism of the specimen was dominated by the sliding of the infill along its bed joints.

The experimental load-displacement behaviour of the specimen and the corresponding hysteresis loops simulated by the Bouc-Wen model are presented in Fig. 5. The Bouc-Wen model, as used in previous studies (Wen 1976, Ma *et al.* 2004), is also applied in this study to simulate the strength and stiffness degradations of MI RC wall panels under successive hysteresis loops. The dynamic response is modelled using a time-marching scheme and the fourth-order Runge-Kutta integration method. The calibrated parameters that resulted in good agreement between the numerical and experimental hysteretic loops are an initial elastic stiffness,  $k = 21.84$  kN/mm, the post-yield elastic stiffness ratio,  $\alpha = 0.005$ , and the other governing parameters:

$A = 1.0$ ,  $\bar{\beta} = 0.75$ ,  $\gamma = -0.5$ ,  $\bar{n} = 1.0$ ,  $\delta_v = 0.0002$ ,  $\delta_\eta = 0.01$ ,  $\zeta_s = 0.8$ ,  $q = 0.001$ ,  $p = 2.0$ ,  $\psi = 0.2$ ,  $\delta_\psi = 0.002$  and  $\bar{\lambda} = 0.1$ .

The numerical hysteretic model of a single panel is subsequently modified to simulate the storey restoring force. A uniform lateral storey stiffness of 740 kN/mm is adopted for the 3-, 5-, and 7-storey models such that the resulting initial fundamental periods ( $T_0$ ) of the structures are consistent with those predicted by Hong and Hwang (2000) for low-rise buildings.

Two hysteretic models, M01 and M02, are created to study the reliability of the proposed analytical ductility relationships when the peak strength is varied and as the stiffness and strength of the hysteretic models degrade. Table 2 summarises some of the general properties of the models.

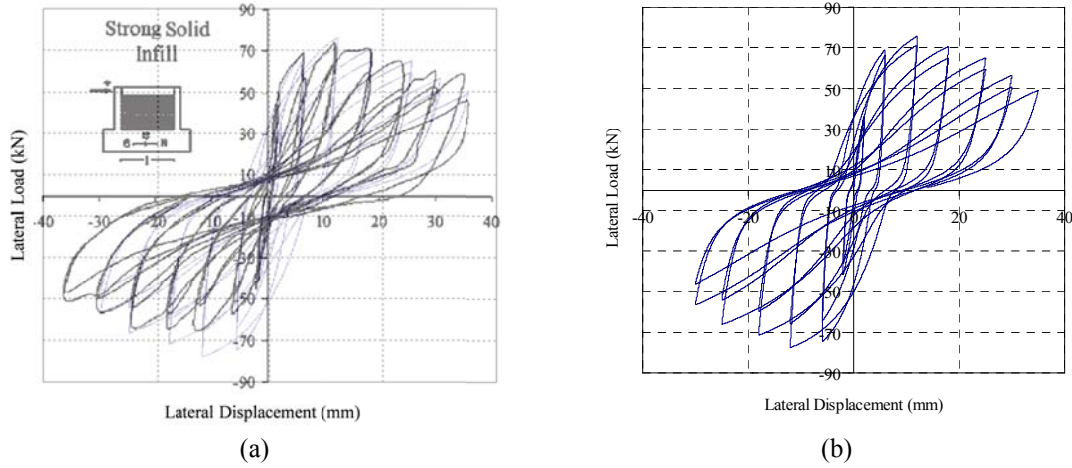


Fig. 5 Lateral load-displacement hysteresis curves: (a) experimental specimen and numerical results and (b) the present numerical model

Table 2 Properties of the MI RC frame models

No. of storeys, $n$	Building height (m)	Model initial period, $T_0$ (sec)	Base shear coefficient at peak strength for hysteretic models	
			M01	M02
3	9	0.15	1.05	0.74
5	15	0.24	0.60	0.43
7	21	0.34	0.42	0.30

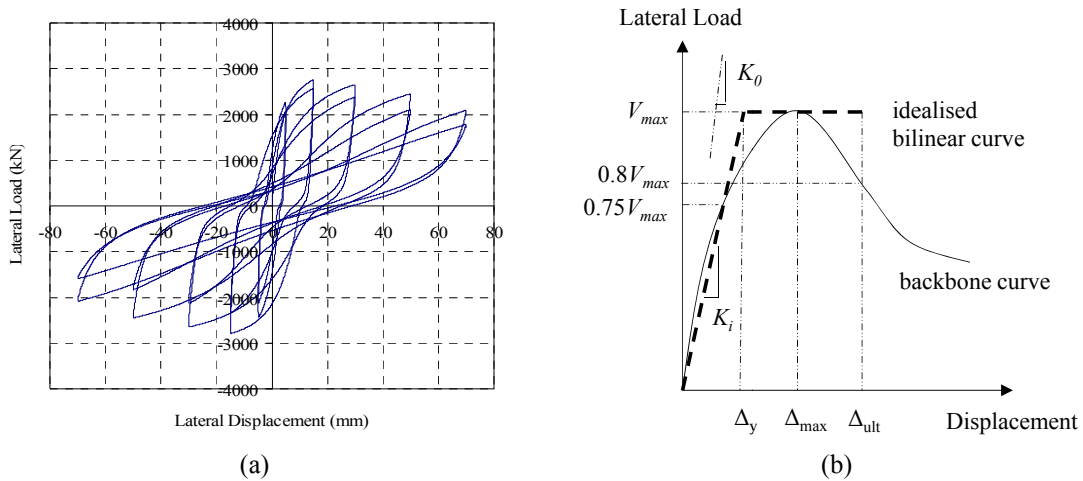


Fig. 6 (a) Interstorey lateral load-displacement hysteresis curve for model M01 and (b) idealised bilinear curve for the load-displacement curve

The first hysteretic model, M01, is shown in Fig. 6(a). An idealised bilinear load-deformation model adopted for defining various damage stages is shown in Fig. 6(b). The lateral displacement

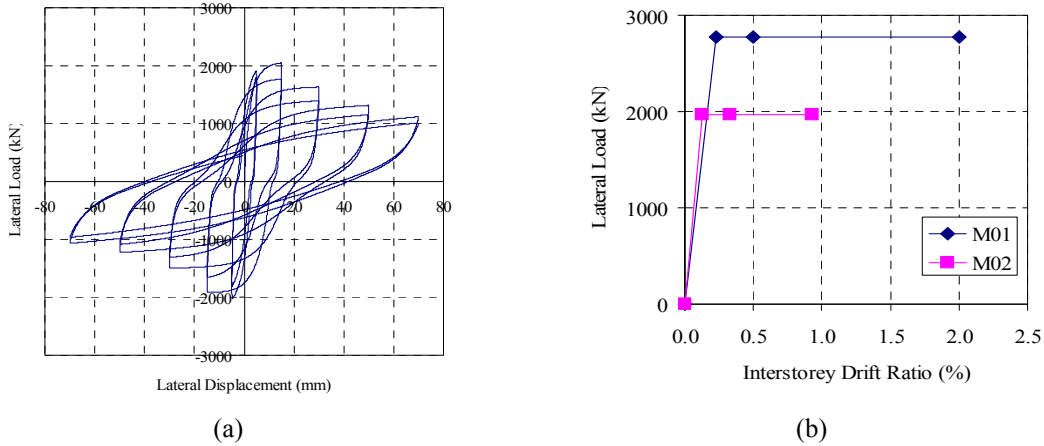


Fig. 7 (a) Interstorey lateral load-displacement hysteresis curve for model M02 and (b) idealised bilinear curves for hysteretic models M01 and M02

( $\Delta$ ) and IDR ( $\theta$ ) of the model, corresponding to various limit states, are as follows: at the yield state,  $\Delta_y = 7$  mm and  $\theta_y = 0.23\%$ ; at the peak load state,  $\Delta_{max} = 15$  mm,  $\theta_{max} = 0.5\%$  and peak strength ( $V_{max}$ ) = 2770 kN; and at the ultimate (collapse) state,  $\Delta_{ult} = 62$  mm and  $\theta_{ult} = 2\%$ . The second model, M02, is constructed to simulate the effects of decreased peak strength and more severe degradations in the post-peak stage. The modified model parameters are  $\gamma = -0.43$  and  $\delta_v = 0.002$ . The resulting lateral displacement and IDR of the model are as follows: at the yield state,  $\Delta_y = 4$  mm and  $\theta_y = 0.13\%$ ; at the peak load state,  $\Delta_{max} = 10$  mm,  $\theta_{max} = 0.33\%$  and peak strength,  $V_{max} = 1970$  kN; and at the ultimate (collapse) state,  $\Delta_{ult} = 28$  mm and  $\theta_{ult} = 0.93\%$ . Fig. 7(a) shows the corresponding hysteresis loops. The evolutions of damage states of the above models are generally comparable to the results obtained on other typical MI RC frame models like Mehrabi *et al.* (1996) which were designed in accordance to American code provisions.

### 3.3 Selected accelerograms

Incremental dynamic analyses are conducted to study the seismic responses of the two building models subjected to 8 different accelerograms of varying intensities. Four of the accelerograms are from strong seismicity regions comprising the El Centro, Kobe, Hachinohe and Northridge earthquakes; the other 4 sets of accelerograms are stochastically generated for low-to-moderate seismicity regions under a return period (RP) of 2,475 years. The accelerograms used in this study include far field and near field earthquakes with various frequency contents and ground motion characteristics. Fig. 8 shows the corresponding acceleration response spectra normalised to peak ground acceleration (PGA) of 0.5 g. The dotted lines in the figures indicate the corresponding approximated first corner period of the ground motions.

## 4. Comparison with incremental dynamic analyses

### 4.1 Results and discussion

IDA are performed for model M01 with 3, 5, and 7 storeys using 8 accelerograms and scaled PGA values from 0.2 g to 1 g with increments from 0.05 g to 0.1 g. From each analysis, the peak displacements at the roof and the first storey are recorded, whilst the yield displacements are obtained from the PO analysis using idealised bilinear models with a triangular load distribution.

Hence, the local and global ductility demands can be derived for each analysis. The numerical ductility relationships computed from the IDA and the predicted results from Eqs. (3), (12) and (13) (as mentioned in Section 2) are shown in Fig. 9. The abbreviations adopted in the figures are as follows: Paulay and Priestley's relationship (Eq. (3)) is denoted by "P", while "Sr" and "St" refer to the results from Eqs. (12) and (13) using rectangular and triangular load distributions, respectively. The symbol "NL" refers to the computed ductility relationships from the suite of input accelerograms. The data considered in this study are limited to local ductility factors from 1 to 6, which should cover the practical range of typical MI RC frames.

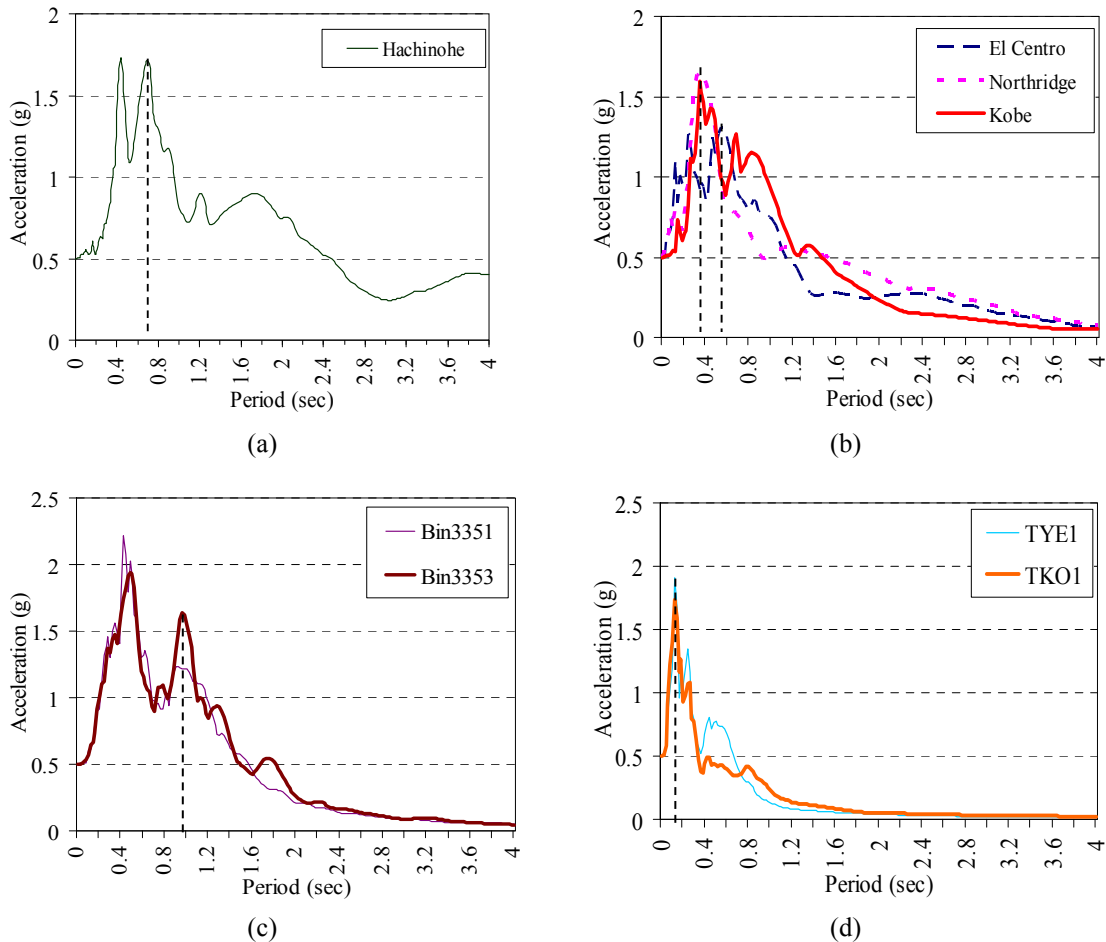


Fig. 8 Normalised acceleration response spectra at 0.5 g for selected accelerograms: (a) from high seismicity regions at far field site, (b) at near field site; stochastically generated accelerograms from low-to-moderate seismicity regions (c) at a far field soil site and (d) at a near field soil site

For all the three analytical ductility relationships, a linear relationship is obtained for the local and global ductility factors. Local ductility is always higher than the global ductility because of the deformation concentration at the first storey. The global ductility predicted by the equations coincides at local ductility factor equal to 1, while their differences increase with the increase in the local ductility factor. For a constant local ductility demand, the relationships from the rectangular load vector and Paulay and Priestley (1992) give the highest and the lowest predicted global ductility demands, respectively. The discrepancies between the predicted results and the numerical results are insignificant for 3-storey buildings (see Fig. 9(a)) and increase with increasing numbers of storeys (see Figs. 9(b) and 9(c)). A consistent trend of increasing global ductility demands with the local ductility demands is observed. The three ductility relationships are probably capable of estimating this increasing trend, with some performing better at different numbers of storeys.

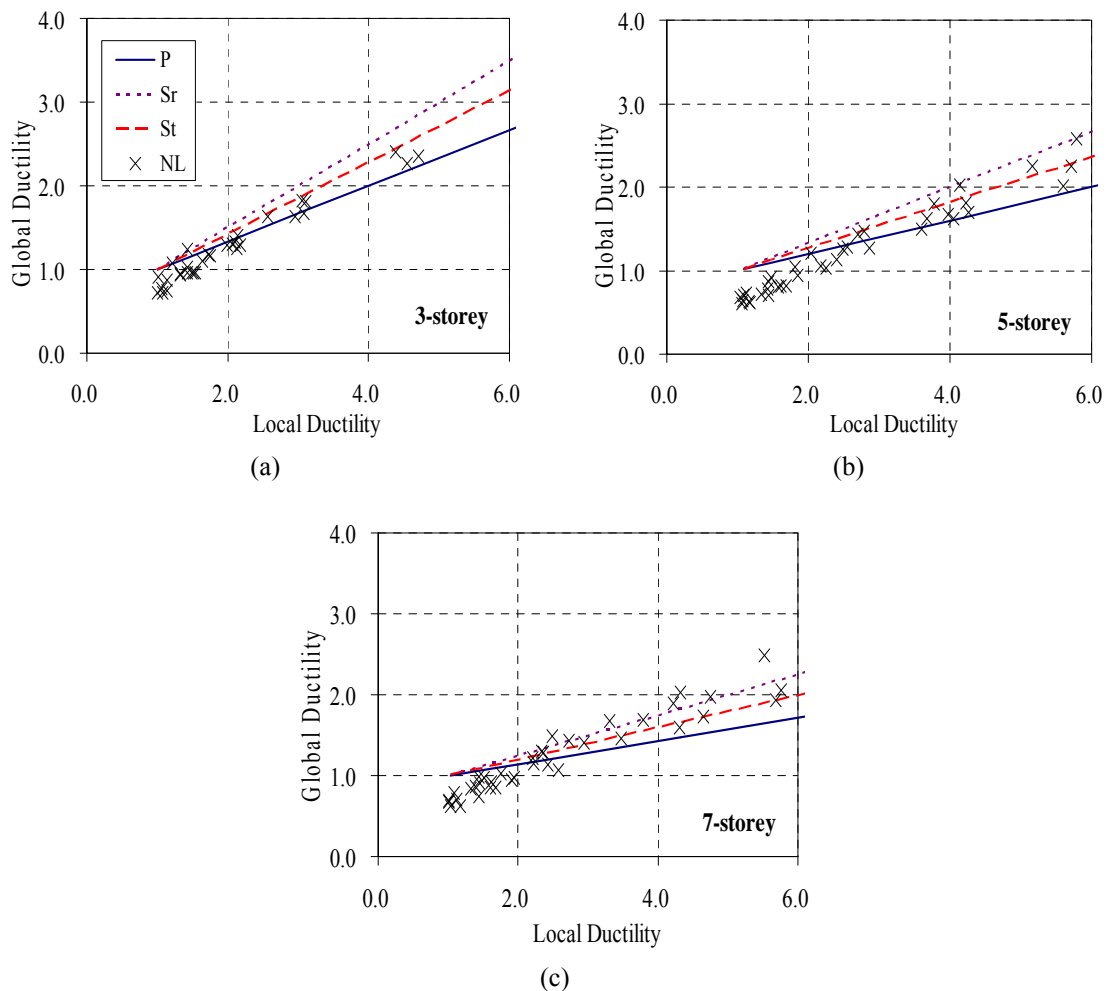


Fig. 9 Global ductility against local ductility from IDA using model M01 and from analytical ductility relationships: (a) 3-storey, (b) 5-storey and (c) 7-storey

The ductility demand relationships from hysteretic model M02 also show similar findings. Fig. 10 shows the global and local ductility demands calculated from the 7-storey building model M02. In general, a degree of scattering of the actual ductility demands is expected when using a large variety of ground motion inputs. Gupta and Krawinkler (2000) suggested that the quality of the PO model, which always yields a unique prediction using a design earthquake, can only be measured by comparing the predicted results to the average of a suite of numerical results from representative earthquakes. Therefore, the averages of absolute percentage errors of the predicted results are presented in Table 3. Paulay and Priestley's relationship is more accurate than the others for 3-storey buildings, while the relationship using the triangular load distribution yields the best overall predictions for 5-, and 7-storey buildings with average absolute percentage errors no greater than 10%. Possible causes for the discrepancies will be discussed in the following sections.

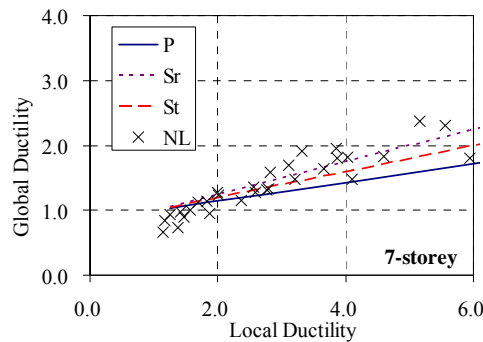


Fig. 10 Local ductility against global ductility from IDA using model M02 and from analytical ductility relationships for 7-storey buildings

Table 3 Absolute percentage errors for the analytical ductility relationships

Hysteretic model	No. of Storeys	Average of absolute % error		
		Linear deflection (P)	Rectangular load (Sr)	Triangular load (St)
M01	3	5	17	10
	5	10	17	10
	7	15	11	10
M02	3	11	11	7
	5	10	15	9
	7	15	9	10
Maximum		15	17	10

Excluding data with local ductility factor < 2 to avoid the influence from low global ductility factor

#### 4.2 Discrepancies in predictions using ductility relationships

As shown in Fig. 9, the global ductility from IDA tends to be higher than the predicted ductility. The first reason is that the post-peak inelastic deformations that occur a few storeys above the first floor are not included in the PO analysis using the simplified bilinear global load-deformation model. Fig. 11 shows the maximum storey displacement envelopes evaluated from IDA. Apart

from the most severe inelastic deformations occurring at the first storey, the interstorey displacements at the upper storeys may also be significantly higher than the notional yield limit of 7 mm for the simplified bilinear model (Fig. 7(b)) and barely exceed the displacement at the peak load state of 15 mm for the hysteretic model, M01. The considerable inelastic deformations at the upper storeys cannot be taken into account by the current PO analysis using the simplified bilinear model. Hence, the inelastic global deformation is underestimated by the PO analysis, so is the global ductility derived from the analytical relationships basing on it.

The second reason is that the accumulation of the residual displacements from successive load cycles also leads to additional deformations in upper storeys. Fig. 12 shows the interstorey shear against storey displacements for a 7-storey building. With higher numbers of storeys and/or increasing local ductility demands by more severe ground motions, buildings experience larger shear demands and higher hysteretic damped energy at upper storeys resulting in more significant strength and stiffness degradation. Hence, smaller non-symmetric reversed cyclic loads could cause inelastic deformations and residual displacements in the upper storeys. The residual displacements also explain why a portion of the storey displacements at upper storeys can be higher than the storey displacement at the peak load state (15 mm), as shown in Fig. 11. Thus, the actual global ductility demands calculated from the IDA are larger than the predictions.

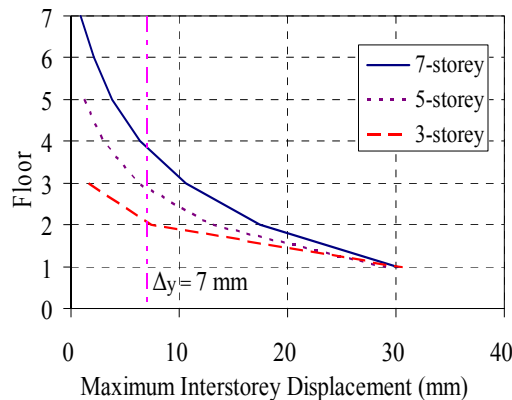


Fig. 11 Maximum interstorey displacements of 3-, 5- and 7-storey buildings for hysteretic model M01 ( $\Delta_y = 7$  mm and  $\Delta_{max} = 15$  mm)

Another discrepancy is the overestimation of the global ductility demands by the analytical ductility relationships for the local ductility factors ranging from 1 to 2. This overestimation can be attributed to the overestimation of the yield roof displacement in PO models from the use of constant storey effective stiffness,  $K_i$ , for all storeys. In fact, the actual storey stiffness decreases gradually as the storey displacement increases. When the local ductility demand is small, the interstorey displacements at the upper storeys are also small. The use of the constant storey effective stiffness,  $K_i$ , for the upper storeys in the PO models likely to underestimate the stiffness and overestimate the storey deformations. Hence, the global ductility demands derived from the IDA are underestimated.

The effects of adopting a different bilinear idealisation model for the ductility relationships of a 7-storey building are shown in Fig. 13. When the undamaged initial elastic stiffness,  $K_0$ , instead of

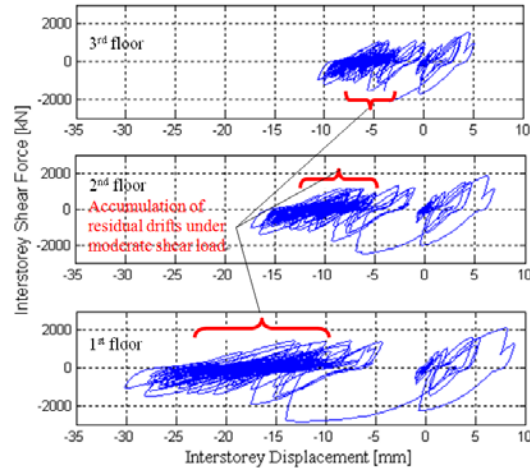


Fig. 12 Interstorey lateral force against displacement curves for a 7-storey building of hysteretic model M01: from (Top) 3<sup>rd</sup> to (Bottom) 1<sup>st</sup> floors

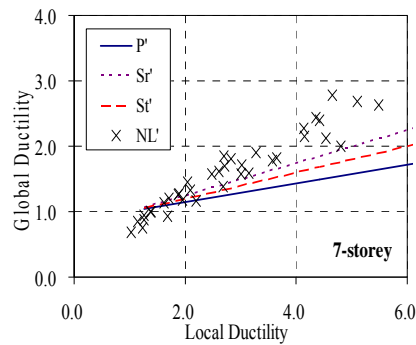


Fig. 13 Local ductility against global ductility from IDA for model M01 and analytical ductility relationships of a 7-storey building using initial undamaged elastic stiffness for bilinear idealisation

the effective stiffness,  $K_i$ , is used in the bilinear model, more accurate predictions are found for low local ductility factors of approximately 1 to 2, but significant overestimation is observed when the local ductility factors are higher than 2. Overall, in the range of local ductility factor from 2 to 6, the bilinear model using the effective stiffness,  $K_i$ , (secant stiffness to the 75% peak strength) can lead to a better approximation of the actual load-displacement behaviour of the storey in the IDA. As a result, the stiffness,  $K_i$ , is adopted in the bilinear model for the PO analysis in the present study.

## 5. Comparison with experimental

The effectiveness of the proposed ductility relationships in facilitating the CBM in evaluating the RSA at the peak load state is described in this section. The selected shake table tests (Kwan and Xia 1996, Negro and Verzeletti 1996, Negro and Colombo 1997, Dolce *et al.* 2005, Stavridis *et*

al. 2011) consist of partial MI RC, uniform MI RC, or pure RC frame models with 3 to 4 storeys and a wide range of geometrical properties, such as single bay (Test Case 1), double bay (Test Case 2-5), or asymmetrical openings (Test Case 3). The layouts of these building models are presented in Fig. 14. They represent buildings conforming to a variety of practices. The models from Test Cases 2, 4 and 5 are designed in accordance to Eurocode 2 and Eurocode 8 with low ductility RC frames except Test Case 4, which is a high ductile frame; whereas, the model from Test Case 1 resembles typical design without specification of adhered standards; the one from Test Case 3 represents construction practice in California in the 1920s and consists of a non-ductile RC frame.

In order to apply the CBM, several input parameters, such as the building height and intact fundamental period, are extracted from the available test information. Table 4 shows a summary of these structural parameters, all of them are converted to prototype values following the law of similitude. For instance, the actual model constructed in Test Case 1 is 4.5 m high with intact fundamental period  $T_0 = 0.130$  sec; with the model scale  $1/S_i = 1/3$ , the 13.5 m high prototype building is estimated to have an intact fundamental period  $= 0.130(S_i)^{1/2} = 0.130(3)^{1/2} = 0.226$  sec as the period similitude factor is not specified in the literature. Other input parameters, including  $\beta_i$ ,  $\theta_y$  and  $\theta_{max}$ , are derived from the hysteresis curves of the first storey of the buildings following the idealisation procedure described in Section 3. Note that for a SDOF system,  $\beta_i$  is equivalent to the square root of the ratio of intact stiffness to idealised stiffness, and same definition is applied here to derive  $\beta_i$  from the stiffness of the first storey. The underlying assumption is that the  $\beta_i$  derived for the first storey is assumed to be equivalent to the  $\beta_i$  of the whole building; however, it could actually be smaller if the upper storeys remain undamaged. In most test cases, the intact storey stiffness is not provided. This value is estimated from the intact period assuming uniform mass and stiffness distribution together with the triangular load distribution. The value of  $\beta_i$  for the five test cases ranges from 1.12 to 1.78, except for Test Case 1, when  $\beta_i = 2.23$ . These values are consistent with the PSF from 1.3 to 1.5 for typical 4- to 7-storey partial MI RC buildings in China (Liang and Chen 2006). Note that  $\beta_i$  exceeds  $\beta$  slightly for Test Cases 1 and 4 which is due to the afore-mentioned reasons together with the close values between the idealised stiffness and the effective stiffness at the peak load state.

The benchmark of experimental results for RSA, PSF and  $\lambda$  are estimated using the dynamic relationships of an equivalent SDOF system, when they are not stated in the literature. For example, the experimental RSA can be derived from the peak acceleration recorded at roof level ( $a_{roof}$ ) using Eq. (18).

Table 4 Summary of structural parameters from experiments

Test case	$n$	Model scale, $1/S_i$	Building height (m)	$T_0$ (sec)	$\beta_i$	$\theta_y$ (%)	$\theta_{max}$ (%)	RSA (g)	$\beta$	$\lambda$
1. MI (Kwan and Xia 1996)	4	1/3	13.50	0.226	2.23	0.55	0.71	0.78	2.12	2.16
2. MI (Dolce <i>et al.</i> 2005)	3	1/3.3	10.64	0.201	1.48	0.31	0.94	1.23	1.94	2.15
3. MI (Stavridis <i>et al.</i> 2011)	3	1/1.5	10.08	0.102	1.12	0.05	1.03	0.87	3.45	3.88
4. Partial MI (1/F RC frame) (Negro and Verzeletti 1996, Negro and Colombo 1997)	4	1/1	12.50	0.599	1.78	1.71	3.50	0.54	1.73	3.04
5. RC frame (Dolce <i>et al.</i> 2005)	3	1/3.3	10.64	0.498	1.48	1.04	1.63	0.50	1.79	1.75

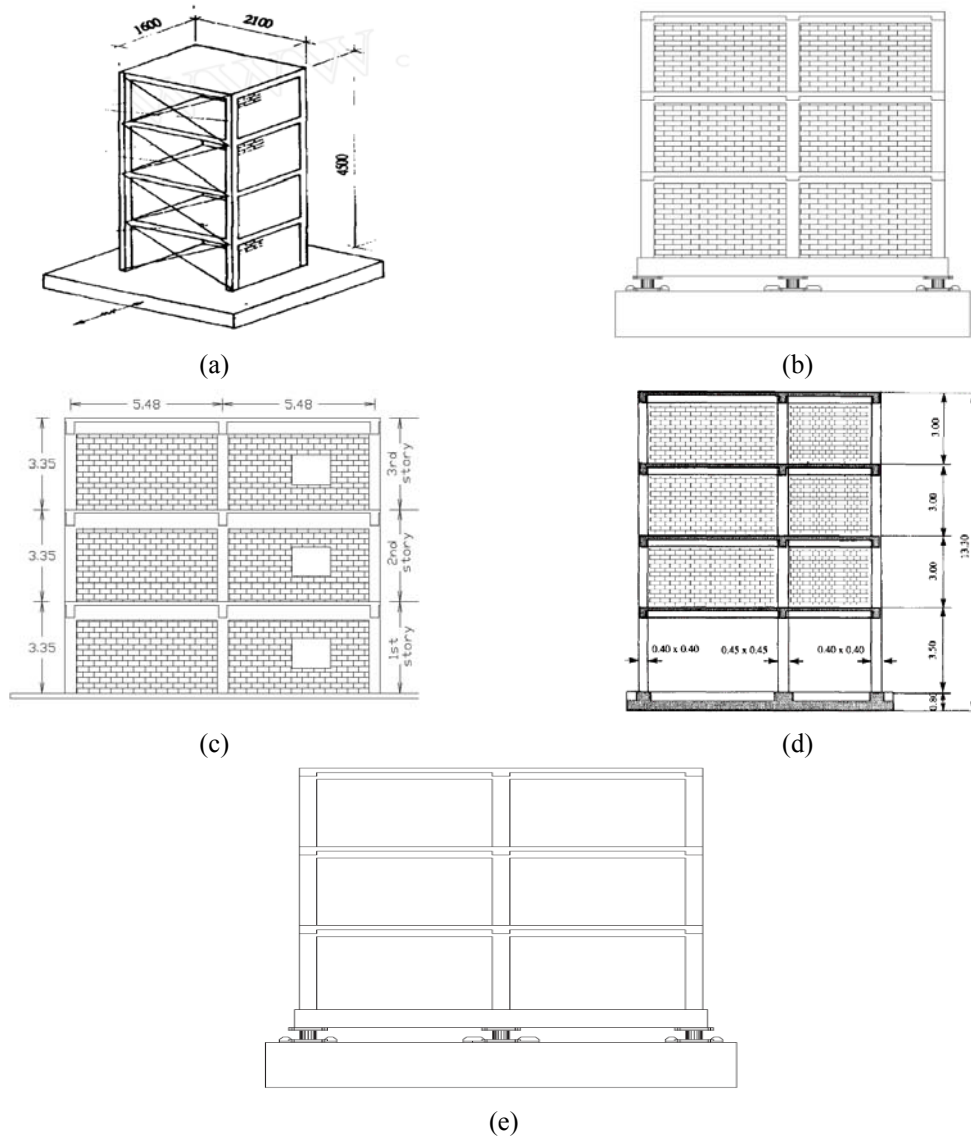


Fig. 14 Building models from other experiments for validation of the coefficient-based method with analytical ductility relationship: (a)-(e) Test Case 1-5, respectively

$$RSA = \frac{1}{\Gamma_1} \frac{a_{roof}}{\phi_{roof,1}} \quad (18)$$

This expression is still approximately correct for structures at an inelastic state dominated by the first vibration mode. By assuming model of uniform mass and stiffness with a triangular load distribution along the building height,  $\Gamma_1$  and  $\phi_{roof,1}$  can be evaluated. For instance,  $a_{roof} = 0.98$  g in Test Case 1, while calculated  $\Gamma_1 \phi_{roof,1} = 1.252$ ; hence, the estimated experimental RSA =

$0.98/1.252 = 0.783$  g. For Test Case 4 (Negro and Verzeletti 1996, Negro and Colombo 1997) which the roof acceleration is not provided, the RSA is derived from the maximum base shear coefficient by assuming the effective mass is equal to 90% of the total mass. Provided the total mass = 336 ton and the peak shear strength = 1.6 MN, the estimated RSA =  $16 \times 10^6 / (0.9 \times 336 \times 10^3 \times 9.81) = 0.539$  g. Apart from the RSA, the experimental PSF is determined by the ratio of effective period at the peak load state over the intact period, which are measured from the Fourier spectra of the structural acceleration response by small intensity vibrations using an impact hammer or during the shake table tests. For Test Case 4, the effective period is undefined. The period is evaluated from the pseudo-RSA and RSD relationship, in which RSD can be estimated from the maximum roof displacement using Eq. (1). Finally, experimental  $\lambda$  can be derived from Eq. (5) given the RSA and PSF.

Based on the above structural parameters, Table 5 shows the predicted RSA, PSF and  $\lambda$  using CBM with the analytical ductility relationship derived from triangular load distribution. For brevity, RSA is predicted from Eqs. (9) and (15), while PSF and  $\lambda$  are predicted from Eqs. (6) and (7), respectively by substituting the global ductility demands with Eq. (13). In general, the predicted RSA, PSF and  $\lambda$  are in good agreement with the experimental results. By normalising the differences relative to the experimental values, their percentage errors are shown in Table 5, in which the underestimation is denoted by a negative sign, and vice versa. Their maximum percentage errors are limited to 22.2%, 19.4% and 18%, respectively. These errors can be attributed to the derivations of the structural parameters as well as the assumptions in the CBM and analytical ductility relationships discussed previously. Apart from uniform MI RC frames, consistent predictions are also observed for Test Cases 5 and 6, a partial MI RC frame building and a RC frame building, respectively. Note that both buildings failed through a soft storey mechanism. This comparison demonstrates the versatility of the analytical ductility relationships that can be applied to different types of regular buildings, as long as the shear deformation mode with soft storey failure mechanism at ground level dominates.

In conclusion, the aforementioned test cases show the applicability of the CBM to predict the seismic behaviour of low-rise regular buildings, provided that the input parameters  $\beta_i$ ,  $\theta_v$  and  $\theta_{max}$  can be correctly estimated. Simplifications in acquiring these input parameters can be derived from generalising the load-displacement curves of confined masonry walls of similar material and geometrical properties (Terán-Gilmore *et al.* 2009); alternatively, probabilistic distributions of the drift ratios with respect to certain damage states can also be created from a database of the experimental tests (Ruiz-García and Negrete 2009). However, due to the limited scope in the present study, prediction of these input parameters for quick seismic assessment is not addressed.

Table 5 Summary of predicted spectral accelerations and other drift related factors

Test Case	RSA (g)	% error	$\beta$	% error	$\lambda$	% error
1. MI (Kwan and Xia 1996)	0.71	-9.9	2.34	10.4	1.97	-8.9
2. MI (Dolce <i>et al.</i> 2005)	0.96	-22.2	2.02	4.4	2.53	18.0
3. MI (Stavridis <i>et al.</i> 2011)	1.00	14.5	3.43	-0.6	3.43	-11.6
4. Partial MI (1/F RC frame) (Negro and Verzeletti 1996, Negro and Colombo 1997)	0.45	-16.0	2.07	19.4	2.54	-16.5
5. RC frame (Dolce <i>et al.</i> 2005)	0.53	4.7	1.65	-8.0	1.97	12.9

## 6. Conclusions

The objective of the study is to establish analytically simple relationships for the global and local ductility demands based on the PO analysis for quick seismic assessments of 3- to 7-storey low-rise regular MI RC buildings with soft storey failure mechanism. Simple analytical ductility relationships are derived from three assumed deflection profiles namely linear deflection profile, and deflection profiles from triangular or rectangular load distributions. The reliability of the relationships is measured by the IDA on 3-, 5-, and 7-storey frame models based on 8 selected accelerograms representing ground motions with various characteristics. Two different hysteretic models are created to study the effects of varying post-peak strength degradation and peak strength on the accuracy of the analytical ductility relationships. Using the ductility relationships and the input parameters  $\beta_i$ ,  $\theta_y$  and  $\theta_{max}$ , RSA and PSF are determined by the CBM and further validated by the shake table test results. Based on this study, the following conclusions are made:

1. Linear local and global ductility relationships can be derived from PO analysis using the bilinear idealisation of the storey load-displacement curve. Among the three ductility relationships studied, the one from the linear deflection profile and from the rectangular load distribution are most accurate for 3- and 7-storey models, respectively; whereas, the ductility relationship from the triangular load distribution provided the best overall estimation for the global ductility from 3- to 7-storey frames with average absolute errors limited to 10% from the IDA.

2. Due to the higher shear force demands, the stiffness degrades more seriously. Upper storeys can undergo inelastic deformations with considerable accumulated residual drifts. Such inelastic and residual deformations can cause the underestimation of the global ductility by the PO analysis.

3. Because the accuracy of the CBM is substantially dependent on the input parameters  $\beta_i$ ,  $\theta_y$  and  $\theta_{max}$ , further studies should be conducted to determine these parameters systematically for new or existing buildings. Nevertheless, this study provides an analytical approach to define the drift factor ( $\lambda$ ) and the PSF ( $\beta$ ) for the CBM. Instead of using constant  $\lambda$  and  $\beta$ , as in previous studies, the present approach is likely to yield better accuracy for the predictions of RSA and RSD, for buildings of up to 7 storeys by fully accounting for the variations in the number of storeys and nonlinearly deflected shapes.

Finally, the analytical local and global ductility relationships developed in this study are able to facilitate the CBM for quick assessments of low-rise regular buildings vulnerable to soft storey failure mechanism at the first storey. Using the analytical ductility relationships with the CBM, the buildings at critical conditions can be effectively identified from groups of existing buildings. This approach provides significant insight into the necessity of more detailed analyses. Allocations of limited resources for remedial actions can thus be better prioritised.

## Acknowledgments

The authors would like to express their gratitude to Dr. H.H. Tsang and final-year undergraduate Mr. V. Ma for providing the stochastically generated accelerograms for the analysis and the two anonymous reviewers for their valuable comments to improve the quality of this paper.

## References

- ATC (1996), ATC-40, *Seismic evaluation and retrofit of concrete buildings, 1-2*, Applied Technology Council (ATC), Redwood City, California, USA.
- China Academy of Building Research. (2008), *Photo collection of 2008 Wenchuan earthquake damage to buildings*, China Architecture & Building Press, Beijing.
- Collins, K.R., Wen, Y.K. and Foutch, D.A. (1996), "Dual-level seismic design: a reliability-based methodology", *Earthq. Eng. Struct. D.*, **25**(12), 1433-1467.
- Dolce, M., Cardone, D., Ponzio, F.C. and Valente, C. (2005), "Shaking table tests on reinforced concrete frames without and with passive control systems", *Earthq. Eng. Struct. D.*, **34**(14), 1687-1717.
- Dolšek, M. and Fajfar, P. (2001), "Soft storey effects in uniformly infilled reinforced concrete frames", *J. Earthq. Eng.*, **5**(1), 1-12.
- Fardipour, M., Lumantarna, E., Lam, N., Wilson, J. and Gad, E. (2011), "Drift demand predictions in low to moderate seismicity regions", *Aust. J. Struct. Eng.*, **11**(3), 195-206.
- Federal Emergency Management Agency (FEMA 356) (2000), *Prestandard and commentary for the seismic rehabilitation of buildings, Report FEMA 356*, Washington D.C., USA.
- Federal Emergency Management Agency (FEMA 440) (2005), *Improvement of nonlinear static seismic analysis procedures, Report FEMA 440*, Washington D.C., USA.
- Foliente, G.C. (1993), *Stochastic dynamic response of wood structural systems, Ph.D. Thesis*, Virginia Polytechnic Institute and State University, Blacksburg, Virginia.
- Gupta, M. and Krawinkler, H. (2000), "Estimation of seismic drift demands for frame structures", *Earthq. Eng. Struct. D.*, **29**(9), 1287-1305.
- Hong, L.L. and Hwang, W.L. (2000), "Empirical formula for fundamental vibration periods of reinforced concrete building in Taiwan", *Earthq. Eng. Struct. D.*, **29**(3), 327-337.
- Kakaletsis, D.J. and Karayannis, C.G. (2008), "Influence of masonry strength and openings on infilled R/C frames under cycling loading", *J. Earthq. Eng.*, **12**(2), 197-221.
- Kwan, A.K.H. and Xia, J.Q. (1996), "Study on seismic behavior of brick masonry infilled reinforced concrete frame structures", *Earthq. Eng. Vib.*, **16**(1), 87-99. (In Chinese)
- Lee, C.L. and Su, R.K.L. (2012), "Fragility analysis of low-rise masonry in-filled reinforced concrete buildings by a coefficient-based spectral acceleration method", *Earthq. Eng. Struct. D.*, **41**(4), 697-713.
- Liang, S.H. and Chen, Z.F. (2006), "Research on the formula of vibration period about masonry structure supported by frame", *Jiangsu Jian Zhu*, **107**(4), 18-20. (In Chinese)
- Lu, Y., Gu, X. and Wei, J. (2009), "Prediction of seismic drifts in multi-story frames with a new storey capacity factor", *Eng. Struct.*, **31**(2), 345-357.
- Ma, F., Zhang, H., Bockstedte, A., Foliente, G.C. and Paevere, P. (2004), "Parameter analysis of the differential model of hysteresis", *J. Appl. Mech. - T. ASME*, **71**(3), 342-349.
- Mehrabi, A.B., Shing, P.B., Shuller, M.P. and Noland, J.L. (1996), "Experimental evaluation of masonry-infilled RC frames", *J. Struct. Eng. - ASCE*, **122**(3), 228-237.
- Miranda, E. (1996), "Assessment of the seismic vulnerability of existing buildings", *Proceedings of the 11th World Conference on Earthquake Engineering, Acapulco, Mexico*, Paper no. 513.
- Miranda, E. (1999), "Approximate seismic lateral deformation demands in multistory buildings", *J. Struct. Eng.*, **125**(4), 417-425.
- Miranda, E. and Reyes, C.J. (2002), "Approximate lateral drift demands in multistory buildings with nonuniform stiffness", *J. Struct. Eng. - ASCE*, **128**(7), 840-849.
- Negro, P. and Colombo, A. (1997), Irregularities induced by nonstructural masonry panels in framed buildings. *Engineering Structures*, **19**(7), 576-585.
- Negro, P. and Verzeletti, G. (1996), "Effect of infills on the global behaviour of R/C frames: energy considerations from pseudodynamic tests", *Earthq. Eng. Struct. D.*, **25**(8), 753-773.
- Paulay, T. and Priestley, M.J.N. (1992), *Seismic design of reinforced concrete and masonry buildings*, John Wiley & Sons, Inc., USA.

- Rodríguez, M. (2005), "Design and evaluation of masonry dwellings in seismic zones", *Earthq. Spectra* **21**, 465-492.
- Ruiz-García, J. and Miranda, E. (2003), "Inelastic displacement ratios for evaluation of existing structures", *Earthq. Eng. Struct. D.*, **32**(8), 1237-1258.
- Ruiz-García, J. and Negrete, M. (2009), "A simplified drift-based assessment procedure for regular confined masonry buildings in seismic regions", *J. Earthq. Eng.*, **13**(4), 520-539.
- Stavridis, A., Koutromanos, I. and Shing, P.B. (2012), "Shake-table tests of a three-story reinforced concrete frame with masonry infill walls", *Earthq. Eng. Struct. D.*, **41**(6), 1089-1108.
- Su, R.K.L. and Zhou, K.J.H. (2009), "Inherent strength-based approach for collapse seismic assessment of low-rise masonry buildings", *Proceedings of the 2009 NZSEE Conference*, Christchurch, New Zealand, 3-5 Apr 2009, 35-42.
- Su, R.K.L., Chandler, A.M., Lee, P.K.K., To, A.P. and Li, J.H. (2003), "Dynamic testing and modelling of existing buildings in Hong Kong", *T. Hong Kong Inst. Engineers*, **10**(2), 17-25.
- Su, R.K.L., Lee, C.L. and Wang, Y.P. (2012), "Seismic spectral acceleration assessment of masonry in-filled reinforced concrete buildings by a coefficient-based method", *Struct. Eng. Mech.*, **41**(4), 1-16.
- Su, R.K.L., Lee, Y.Y., Lee, C.L. and Ho, J.C.M. (2011), "Typical collapse modes of confined masonry buildings under strong earthquakes", *Open Constr. Build. Technol. J.*, **5**(Suppl. 1-M2), 50-60.
- Sucuoglu, H. and Yazgan, U. (2003), *Simple survey procedures for seismic risk assessment in urban building stocks, seismic assessment and rehabilitation of existing buildings*, NATO Science Series IV/29, 97-118.
- Terán-Gilmore, A., Zuñiga-Cuevas, O. and Ruiz-García J. (2009), "Displacement-based seismic assessment of low-height confined masonry buildings", *Earthq. Spectra*, **25**(2), 439-464.
- Tomažević, M. and Klemenc, I. (1997), "Verification of seismic resistance of confined masonry buildings", *Earthq. Eng. Struct. D.*, **26**(10), 1073-1088.
- Tsang, H.H., Su, R.K.L., Lam, N.T.K. and Lo, S.H. (2009), "Rapid assessment of seismic demand in existing building structures", *Struct. Des. Tall Spec.*, **18**(4), 427-439.
- Wen, Y.K. (1976), "Method for random vibration of hysteretic systems", *J. Eng. Mech.- ASCE*, **102**(2), 249-263.
- Zheng, S.S., Yang, Y. and Zhao, H.T. (2004), "Experimental study on seismic behavior of masonry building with frame – shear wall structure at lower stories", *China Civil Eng. J.*, **37**(5), 23-31.
- Zhu, Y., Su, R.K.L. and Zhou, F.L. (2007), "Cursory seismic drift assessment for buildings in moderate seismicity regions", *Earthq. Eng. Vib.*, **6**(1), 85-97.

IT